Brain Tumor Target Volume Segmentation: Local Region Based Approach

Mehdi Astaraki[1], Hossein Aslian[2]

[1]IAU Science and Research branch, Department of Biomedical Engineering, Tehran, Iran
[2]International Centre for Theoretical Physics (ICTP) and University of Trieste, Department of Medical Physics, Trieste, Italy

Abstract— **In this paper, we comprehensively evaluated clinical application of local robust-region based algorithms to delineate the brain target volumes in radiation therapy treatment planning. Localized region based algorithms can optimize processing time of manual target tumor delineation and have perfect correlation with manual delineation defined by oncologist due to high deformability. Accordingly, they can receive much attention in radiation therapy treatment planning. Firstly, clinical target volumes (CTVs) of 135 slices in 18 patients were manually defined by two oncologists and the average of these contours considered as references in order to compare with semi-automatic results from different four algorithms. Then, four localized region based algorithms named Localizing Region Based Active Contour (LRBAC), Local Chan-Vese Model (LCV), Local Region Chan-Vese Model (LRCV) and Local Gaussian Distribution Fitting (LGDF) were applied to outline CTVs. Finally, comparisons between semi-automatic results and baselines were done according to three different metric criteria: Dice coefficient, Hausdorff distance, and mean absolute distance. Manual delineation processing times of target tumors were also performed. Our result showed that LCV has advantage over other algorithms in terms of the processing time and afterward LRCV is the second fastest method. LRBAC was the second slowest technique; however, we found that processing speed in LRBAC can be almost doubled by replacing the time-consuming re-initialization process with energy penalizing term. Accordingly, due to high accuracy performance of LRBAC algorithm, it can be concluded that the modified version of LRBAC has the best performance in brain target volumes in radiation therapy treatment planning among other localized algorithms in terms of speed and accuracy.**

Keywords— **Brain Tumor Target, Segmentation, region-based, active contour, Treatment Planning.**

I. Introduction

Brain tumor segmentation provides decisive information about the shape, volume and exact location of the patient tumor which is a vital step in treatment planning and diagnosis as well. The more precise and accurate delineation will ultimately result in more effective treatment [1,2]. Additionally, MRI based target volume delineation received more attention due to the fact that contouring brain tumors from CT images is a challenging process. Though quite a few segmentation methods have been proposed, in a general view medical image segmentation can be classified into three categories: manual, automatic and semi-automatic. In manual delineation the tumor regions should be localized slice by slice which is strongly time consuming and depends upon the human experience. Unlike the manual methods, there is no any interaction between the experts and the software in automatic segmentation methods. These methods often need a set of training images to learn the tumor features; and since the tumor properties varies from case to case, learning all feasible features from a finite training set is impossible accordingly. Moreover, automatic method mostly used the Post Contrast T1 Weighted images; therefore, they are not able to detect heterogeneous tumors [3,4]. However, in semi-automatic methods usually an expert sets the initial parameters and control the segmentation procedure. Hence, these techniques could be more reliable in target volume delineation where clinical judgment is highly required.

One of the most successful and well-established class of image segmentation methods is active contour models. These models first introduced by Kass et.al and improved very extensively based on the PDE based level set method proposed by Osher et.al [5,6]. Some of the unique properties of this method are: sub-pixel accuracy, split & merging, topology changes. The main idea behind these models is to evolve an initial closed curve toward the boundaries of target via minimizing an energy functional. These energies can be categorized into two major classes: edge-based [7,8] and region-based [9,10]. In medical and cancer imaging, it is better not to use edge-based methods due to low contrast and weak edges of images. Another equally important reason is that using global image statistics in images with intensity inhomogeneity leads to unsatisfactory results. To cope with this problem many researchers proposed to use the local image statistics in region-based methods [11,12]. Correspondingly, a very robust region based method was clinically evaluated in radiotherapy treatment planning and demonstrated the potential clinical use of region-based segmentation algorithms in radiation therapy [1].

In this paper, we first evaluate four well-known local region-based energy functional for segmenting brain tumor targets and then compare the results in terms of processing time and correlation with manual references. Finally, we remove the very time consuming re-initialization process from the most accurate functional to improve time-efficiency

D.A. Jaffray (ed.), *World Congress on Medical Physics and Biomedical Engineering, June 7-12, 2015, Toronto, Canada*,
IFMBE Proceedings 51, DOI: 10.1007/978-3-319-19387-8_47

and to the best of our knowledge, this modification has not been done yet.

II. Materials and method

A. Experimental Data

The MR images used in this research contain 135 image slices from 18 different patients. These images acquired from 1.5 Tesla Magneton Avanto (Siemens medical system, Erlage, Germany) and 1.5 Tesla GE Sigma Horizon (GE medical, Milwaukee, WI). The image properties are as follow: FLAIR and T2 weighted MRI, spatial resolution of 256×256 pixel, axial view, $4 - 5mm$ slice thickness, $5 - 6mm$ slice gap and 200:240mm FOV.

B. Segmentation Energy Functionals

a) Localizing Region Based Active Contour (*LRBAC)*

This energy is based on the average intensity inside and outside of a local window at every point of the zero level function. The level set function is initialized to be a signed distance function and it needs a re-initialization process at each iteration to prevent the zero level set of being too flat or steep [11].

$$\frac{\partial \varphi}{\partial t}(\mathrm{x}) = \delta\big(\varphi(\mathrm{x})\big)[\int B(\mathrm{x},\mathrm{y})\nabla F(I,\varphi,\mathrm{y})d\mathrm{y} + Reg(\varphi)] \quad (1)$$

$$F(I,\varphi,\mathrm{y}) = H\big(\varphi(y)\big)(I(y)-c_1)^2\left(1-H\big(\varphi(y)\big)\right)(I(y)-c_2)^2 \quad (2)$$

In the above equation, c_1 and c_2 refer to average image intensity inside and outside of the local window respectively. Also, for the rest of the paper I denotes the main image, φ is the level set function, $H(.)$ is Heaviside function, $\delta(.)$ is Dirac Delta function and Reg refers to length minimization energy.

b) Local Chan-Vese Model (*LCV)*

The basic idea of this energy is subtracting the image from its smoothed version which increase the contrast between the objects and background.

$$\frac{\partial \varphi}{\partial t}(\mathrm{x}) = \delta\big(\varphi(\mathrm{x})\big)[|g_k * I(\mathrm{x}) - I(\mathrm{x}) - d_1|^2 + |g_k * I(\mathrm{x}) - I(\mathrm{x}) - d_2|^2 + Reg(\varphi)] \quad (3)$$

In this equation, g_k is an averaging mask with the size of $k \times k$, $*$ denotes the convolution operator and d_1 and d_2 are two global averages image intensity but calculated from the contrast enhanced image [13].

c) Local Region Chan-Vese Model (*LRCV)*

This energy model inspired by the Region Scalable Fitting model [12]. However, unlike the two mentioned algorithms, this algorithm uses spatially varying image intensity [14].

$$\frac{\partial \varphi}{\partial t}(\mathrm{x}) = \delta\big(\varphi(\mathrm{x})\big)[(I(\mathrm{x}) - c_1(\mathrm{x}))^2 + (I(\mathrm{x}) - c_2(\mathrm{x}))^2 + Reg(\varphi)] \quad (4)$$

d) Local Gaussian Distribution Fitting *(LGDF)*

This functional uses spatially varying standard deviation and average image intensity in a Gaussian framework [15].

$$\frac{\partial \varphi}{\partial t}(\mathrm{x}) = \delta\big(\varphi(\mathrm{x})\big)[(e_1 - e_2) + Reg(\varphi)] \quad (5)$$

$$e_i(x) = \int w(y-x)\left[log\big(\sigma_i(y)\big) + \frac{\big(c_i(y)-I(x)\big)^2}{2\sigma_i^2(y)}\right]dy\,;\, i = 1,2 \quad (6)$$

In the last equation, c_i and σ_i denote the average and standard deviation respectively and $w(.)$ refers to localizing Gaussian kernel.

e) Modified LRBAC

Except LRBAC, Level set functions in all other algorithms are initialized with a step binary function and their re-initialization process is replaced by a Gaussian filtering or laplacian operator. For removing the PDE based re-initialization procedure in LRBAC function, we use a very fast and stable energy term named 'Reaction Diffusion' proposed by K.Zhang [16] and we modify the algorithm as below:

1. Initialize φ as a step binary function:±3
2. Calculate evolution equation (eq.1)
3. Smooth the level set function via diffusion term.
4. Check for convergence criteria (If satisfied; stop, otherwise back to step2).

C. Brain tumor segmentation

The segmentation procedure consists of following steps. First the initial contour around the tumor region is drawn by selecting 3 to 6 points, depending on the complexity of tumor geometry. Owing to the fact that the initial contour evolves following its normal direction using image statistics, there is no limit to set the initial contour in or out of the tumor region.

It has to be noted that all five algorithms are initialized to the same selecting points for each image slice (as shown in Fig. 1). Finally, the tumor volumes from all these semiautomatic algorithms are obtained considering the slice thicknesses and slice gaps.

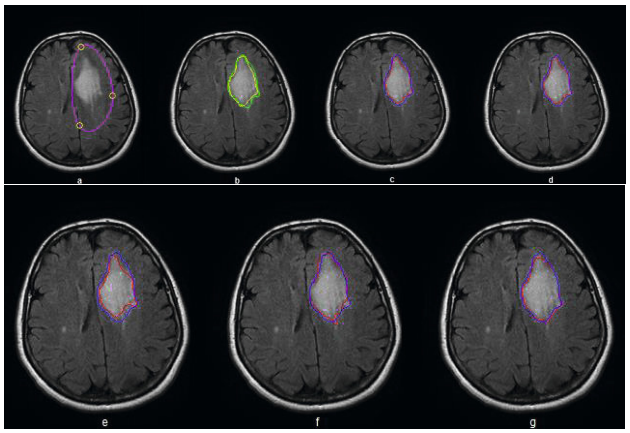

Fig. 1 a) initial contour by 3 points, b) two manual expert delineation, c:g) average of two experts' contours in blue and the final result of LRBAC, modified LRBAC, LRCV, LCV and LGDF respectively in red.

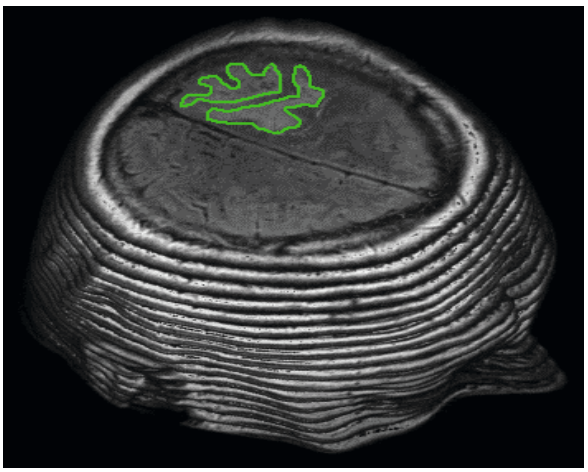

Fig. 2 Reconstructed volumetric image

III. Results

To evaluate the accuracy of algorithms, the segmentation results are compared with manual reference contours drawn by two different experts using three error metric: one similarity measure 'Dice coefficient' and two dissimilarity measures 'Mean Absolute Distance' and 'Hausdorff distance' [17]. Table 1 indicates the mean values obtained from all image slices and table 2 depicts the ratio of estimated tumor volume to the manual volume for two random cases.

Table 1 The mean value of error metrics and average computational time for each slice

Algorithm	Dice	MAD (cm)	HD (cm)	Contouring Time for each slice (sec)
LRBAC	0.919 ±0.31	0.13± 0.32	0.29± 0.91	13.12± 7.79
Modified LRBAC	0.912 ±0.27	0.14± 0.34	037± 0.22	8.14± 6.14
LCV	0.83 ±0.42	0.27± 0.71	0.52± 0.28	5.87± 3.62
LRCV	0.82 ±0.32	0.26± 0.45	0.55± 0.14	19.65± 11.56
LGDF	0.91 ±0.34	0.13± 0.35	0.37± 0.95	9.16± 3.13

IV. Discussion

As can be seen from Table 1, the LCV is the fastest among the others, however this method and LRCV are the less accurate. In LCV a high pass filtering use to enhance the image contrast. However, applying this filter does have a noticeable drawback leading to the loss of the tumor's outer edge. This might happen, if the contrast between tumor and its adjacent tissue is low. In addition, LCV and LRCV have serious challenge to set the regularization parameters which depend on the image resolution, image contrast and tumor size; therefore, selecting the proper parameters varies for each images. The other issue of these two algorithm is their high sensitivity to initial contour.

Although LGDF uses both standard deviation and intensity averages, tumor region statistical and background are not necessarily followed by Gaussian distribution.

In LRBAC, the only required parameter to set is the radius of a local window which is selected with regards to the distance between initial contour and tumor boundaries and the distance between tumor and its nearby tissue. As mentioned in the previous section, in order to improve time consuming re-initialization procedure in LRBAC, which is considered as the main disadvantage of this method, the modified LRBAC version was evaluated and its performance was satisfactory in this application.

It should be noted here that all these algorithms could localize the gross target volume, if GTV is palpable and visible in the images.

V. Conclusion and future work

In this work we investigated and compared the performance of different local region based active contour techniques to obtain brain tumor target volume. For this purpose, we used four well known algorithm which are robust to intensity inhomogeneity and have high deformability. Of all these localized region based algorithms, LRBAC has the best accuracy; however, it is the second slowest. Therefore, to reduce the processing time we proposed a modified version for this algorithm and this could improve the time efficiency up to 40%. Conclusively, as for appropriate accuracy of LRBAC algorithm, the modified version can be more suitable in brain target volumes in radiation therapy treatment planning and has a more balanced compromise between speed and accuracy.

For future study, another comprehensive work can be performed to evaluate these localized segmentation techniques in other important organs and compare the results as well. Also, using fused images instead of just MRI images and analyze strengths and weakness of each method in each specific organ can be addressed for the future works.

Table 2 The ratio of tumor volume estimated to the manual calculated volume for two different cases

Tumor Volume Ration (semi-automatic/manual)						
Case	# of slice	LRBAC	modified LRBAC	LCV	LRCV	LGDF
1	9	0.926	0.914	0.845	0.827	0.921
2	12	0.892	0.887	0.786	0.763	0.876

Acknowledgment

The authors would like to express their upmost gratitude to Professors Mahdi Sadeghi, Seied Rabi Mahdavi and Pedram Fadavi for their valuable guidance.

Reference

1. Aslian H, Sadeghi M, Mahdavi Sr et al. (2013) Magnetic resonance imaging-based target volume delineation in radiation therapy treatment planning for brain tumors using localized region-based active contour. Int J Radiat Oncol Biol Phys 87: 195-201.
2. Rank Ch M, Hünemoh**r** N, Naghel Nagel A M et al. (2013) MRI-based simulation of treatment plans for ion radiotherapy in the brain region. Radiotherapy and Oncology 109:414–418.
3. Njeh I, Sallemi L, Ben Ayed I et al. (2014) 3D multimodal MRI brain glioma tumor and edema segmentation: a graph cut distribution matching approach. Computer Medical Imaging and Graphics “in press”.
4. Sachdeva J, Kumar V, Gupta I et al. (2012) A novel content based active contour model for brain tumor segmentation. Magn Reson Imaging 30:694-715.
5. Kass M, Witkin A, Terzopoulos D (1988) Snakes: Active contour models. Int J Comput Vision; 1:321-331.
6. Osher S, Sethian Ja (1998) Fronts propagating with curvature-dependent speed: Algorithms based on Hamilton-Jacobi formulations. J Comput Phys 79:12-49.
7. Caselles V, Kimmel R, Sapiro G (1997) Geodesic active contours. International Journal of Computer Vision 22:61-79.
8. Paragios N, Deriche R (2000) Geodesic active contour and level sets for the detection and tracking of moving objects. IEEE Trans. Patt. Anal. Mach. Intel 22:266-280.
9. Chan Tf, Vese La (2001) Active contours without edges. IEEE T Image Process 10:266-277
10. Zhang K, Song H, Zhou W (2010) Active contours with selective local or global segmentation: A new formulation and level set method. Image and Vision computing 28: 668-676.
11. Lankton Sh, Tannenbaum T (2008) Localizing region-based active contours. IEEE T Image Process 17:2029-2039.
12. Li Ch, Kao Ch Y, Gore J C et al. (2008) Minimization of region scalable fitting energy for image segmentation. IEEE T Image Process 17:1940–1949.
13. Wang Xi F, Huang De Sh, Xu H (2010) An Efficient Local Chan-Vese Model for Image Segmentation. Pattern Recognition. 43:603-618.
14. Liu Sh, Peng Yali (2012) A local region-based Chan-Vese model for image segmentation. Pattern Recognition 45:2769-2779.
15. Wang L, He L, Mishra A et al. (2009) Active contours driven by local Gaussian distribution fitting energy. Signal Processing 89:2435-2447.
16. Zhang K, Zhang L, Song H, et al. (2012) Re-initialization-free level set evolution via Reaction Diffusion. IEEE T Image Process 22:258-271.
17. Dietenbeck T1, Alessandrini M, Barbosa D et al. (2012) Detection of the whole myocardium in 2D-echocardiography for multiple orientation using a geometrically constrained level- set. Med. Img Anal. 16:386-401.

Author: Hossein Aslian
Institute: International Centre for Theoretical Physics (ICTP) and University of Trieste
Street: ICTP - Strada Costiera, 11 I - 34151
City: Trieste
Country: Italy
Email: aslian@ictp.it